

Supporting Information

Preparation of meso-porous aromatic frameworks for rapid ion extraction from high salt and corrosion environments

Cheng Zhang,^{a,†} Huanhuan Li,^{a,†} Doudou Cao,^a Yingbo Song,^a Yue Zheng,^a Jiarui Cao,^a Wanying Chen,^a Yuan Ye,^a Nan Gao,^{a,*} and Yajie Yang^{a,b,*}

^a Key Laboratory of Polyoxometalate and Reticular Material Chemistry of Ministry of Education, Northeast Normal University, Changchun, 130024, China

^b Key Laboratory of Automobile Materials of Ministry of Education & School of Materials Science and Engineering, Jilin University, Changchun 130022, China

[†] Equally contributed to this work.

*Correspondence: gaon320@nenu.edu.cn, yangyajie@jlu.edu.cn

Table of Contents

Experimental procedures	3
Materials and general instrumentation	3
Synthesis	4
Synthesis of PAF-174 and PAF-175-AO.....	4
Methods.....	5
Results and Discussion	7
Characterization	7
References.....	20

Experimental

Materials

Triethylamine, silicon dioxide, tetraethyl orthosilicate (TEOS), resorcinol, parabens, biphenyldicarboxaldehyde, 3-formyl-4-hydroxybenzotrile, and hydrofluoric acid were purchased from Anegi Chemical Reagent Co. Ethanol, trichloromethane, and tetrahydrofuran were purchased from Beijing Chemical Plant Reagent Co. Ferric nitrate ($\text{Fe}(\text{NO}_3)_3 \cdot 9\text{H}_2\text{O}$), sodium nitrate (NaNO_3), magnesium nitrate ($\text{Mg}(\text{NO}_3)_2$), potassium nitrate (KNO_3), zinc nitrate ($\text{Zn}(\text{NO}_3)_2 \cdot 6\text{H}_2\text{O}$), calcium nitrate ($\text{Ca}(\text{NO}_3)_2 \cdot 4\text{H}_2\text{O}$), sodium vanadate (NaVO_3), and lithium nitrate (LiNO_3) were purchased from the Beijing Chemical Industry Reagent Company. Uranyl nitrate hexahydrate was purchased from Beijing Pharmaceutical Company.

General instrumentation

Fourier transform infrared spectroscopy (FTIR) was carried out on a Nicolet Impact 410. Powder x-ray diffraction (PXRD) was performed on a Bruker D8 QUEST diffractometer with Cu-K α radiation. Thermo-gravimetric analysis (TGA) was recorded by a METTLER TOLEDO TGA/DSC 2 thermal analyzer under an air atmosphere at a heating rate of 10 °C min⁻¹. Scanning electron microscope (SEM) was conducted on the JEOS JSM 6700. Transmission electron microscope (TEM) was obtained on a JEM-2100 with an accelerating voltage of 200 kV. X-ray photoelectron spectroscopy (XPS) was implemented on the AXIS ULTRA. N₂ adsorption-desorption measurement was tested on a Quantachrome Auto-sorb. UV-Vis absorption spectra were conducted with a spectrophotometer (Cary500, VARIAN, America). Inductively coupled plasma atomic emission spectrometer (ICP-AES) was recorded on the Teledyne Leeman Labs Prodigy. Inductively coupled plasma mass spectrometry (ICP-MS) was recorded on the PerkinElmer Optima 3300DV. U L3 edge XAFS spectra were collected at the beamline 14W1 in the Shanghai Synchrotron Radiation Facility, a 3.5 GeV third-generation synchrotron source. The raw absorption data were first background subtracted by fitting the pre-edge using a least-squares method, and then normalized to one at energies far from the edge. All the spectra were processed using the WinXAS version 3.1 Program. Simulations of the EXAFS scattering paths to fit experimental data were calculated with the FEFF6 code.

Synthesis

Synthesis of PAF-174-AO and PAF-175-AO.

1.6 g silica and 2.0 g TEOS (ethyl orthosilicate) were dissolved in a solution of 20.0 g ethanol and 1.0 g hydrochloric acid (0.1 M). Then, 0.504 g (4 mmol) resorcinol, 3.0 mmol benzaldehyde (terephthalaldehyde or biphenyldicarboxaldehyde), and 0.4945 g (3.3613 mmol) 3-formyl-4 hydroxybenzotrile were added. The products were obtained as PAF-174-SiO₂ and PAF-175-SiO₂, respectively, after stirring for 1 h and heat treatment at 100 °C for 24 h. The products were subsequently solvated with tetrahydrofuran and trichloromethane for 48 h, respectively.

To remove silica, the samples were immersed in 5% HF solution for 24 h × 2 times, and then the samples were thoroughly rinsed and dried in an oven at 100 °C overnight. The solids were named PAF-174 and PAF-175, respectively.

The samples were then amidoximized by adding 100 mg samples (PAF-174 and PAF-175), 400 mg hydroxylamine hydrochloride, 700 μL triethylamine, and 10 mL ethanol in a 25 mL flask at room temperature and heated in an oil bath at 70 °C for 48 h. After the reaction, the samples were cooled down to room temperature, filtered by pumping, and then the solids were rinsed on the filter paper with deionized water. The solid was put into 100 mL 1 M Na₂CO₃ alkaline solution and stirred for 24 h for alkaline treatment. The samples PAF-174-AO and PAF-175-AO were dried under vacuum in an oil bath at 70 °C for 12 h. After the reaction was completed, the sample was cooled to room temperature and rinsed with deionized water.

Methods

Adsorption capacity test.

A solution of uranium ions at a concentration of 10 ppm was prepared by dissolving $\text{UO}_2(\text{NO}_3)_2 \cdot 6\text{H}_2\text{O}$ in deionized water. During the adsorption process, the system was stirred to maintain the homogeneity of the ions in the solution. The adsorption capacity of the adsorbent material for uranyl ions was recorded at intervals of 5, 10, 15, 30, 60, 120, 180, 240, 300, and 360 minutes.

Calculation for adsorption capacity.

$$Q_e = (C_0 - C_e) \frac{V}{M}$$

Q_e is the adsorption capacity at the adsorption equilibrium (mg g^{-1}), C_0 is the initial concentration (ppm), C_e is the equilibrium concentration (ppm), V is the volume of the adsorption system (L), and M is the mass of the adsorption material (mg).

Ion selectivity test.

The selectivity of PAF-174-AO for uranyl species in the presence of different metal ions was investigated in beakers containing about 10 ppm of UO_2^{2+} , VO_3^- , Fe^{3+} , Cu^{2+} , K^+ , Ca^{2+} , Na^+ , Mg^{2+} , Zn^{2+} , and Ni^{2+} . After the contact for 6 h, ICP-AES was adopted to detect the concentration changes of metal ions in the solution. The selectivity coefficient of the PAF-174-AO was calculated using the formula below:

$$K_{(U/M)} = \frac{Q_{(U)}}{Q_{(M)}} \times 100\%$$

$Q_{(U)}$ is the adsorption capacity of uranyl ions (mg g^{-1}), $Q_{(M)}$ is the adsorption capacity of metal ion M (mg g^{-1}), and $K_{(U/M)}$ is the selectivity coefficient of the PAF-174-AO.

Recycle test.

To elute uranyl ions from the uranium-adsorbed PAF-174-AO, the material was suspended in 100 mL of eluent (1 M, NaHCO_3) for 1 hour. The process was repeated twice and the material was washed with water and dried to study the cycling performance of PAF-174-AO.

Adsorption kinetics.

The adsorption isotherm of PAF-174-AO and PAF-175-AO for uranyl ions was fitted using the respective *pseudo-first-order* and *pseudo-second-order* dynamic models. The *pseudo-first-order* model is described as follows:

$$\ln(Q_e - Q_t) = \ln(Q_e) - K_1 t$$

Q_t is the adsorption capacity at the time t (min) (mg g^{-1}), Q_e is the adsorption capacity of the material at the adsorption equilibrium (mg g^{-1}), and K_1 is the *pseudo-first-order* kinetic constant (min^{-1}).

The *pseudo-second-order* dynamic model is described as follows:

$$\frac{t}{Q_t} = \frac{1}{K_2 Q_e^2} + \frac{t}{Q_e}$$

Q_t is the adsorption capacity at the time t (min) (mg g^{-1}), Q_e is the adsorption capacity of the material at the adsorption equilibrium (mg g^{-1}), and K_2 is the rate constant ($\text{g mg}^{-1} \text{min}^{-1}$).

The binding affinity of PAF-174-AO for metal ions is investigated with the distribution coefficient, using the

following equation.

$$K_d = \frac{C_0 - C_e}{C_e} \times \frac{V}{M}$$

C_0 is the initial concentration (ppm), C_e is the equilibrium concentration (ppm), V is the volume of the adsorption system (mL), M is the mass of the PAF-174-AO material (g), and K_d is the distribution coefficient.

Seawater adsorption experiment.

The PAF-174-AO 5mg was tested in a beaker containing a total of 100 L real seawater, circuited continuously by the peristaltic pump with a flow rate of 80 mL min⁻¹. The capacity of PAF-174-AO for uranyl ions was recorded at an interval time of 3, 5, 10, 15, and 20 days using ICP-MS measurement.

Result and Discussion

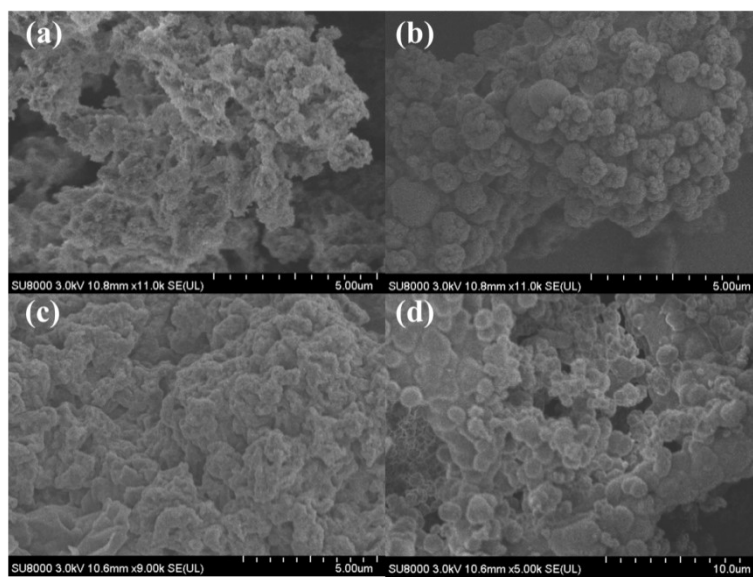


Figure S1. SEM images of PAF-174 (a), PAF-175 (b), PAF-174-AO (c), and PAF-175-AO (d).

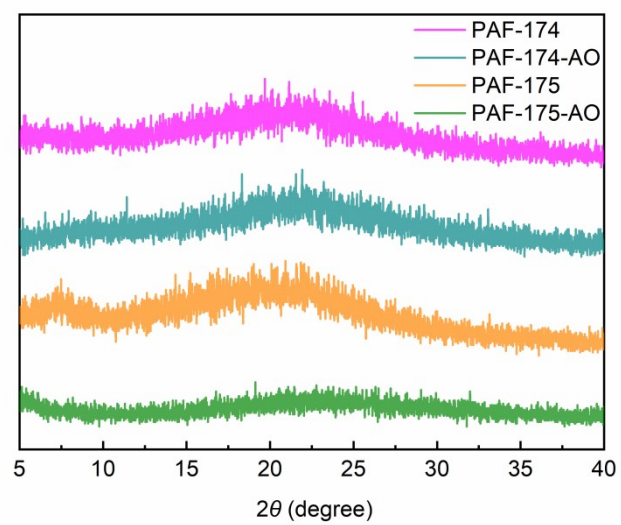


Figure S2. PXRD patterns of PAF-174, PAF-174-AO, PAF-175, and PAF-175-AO.

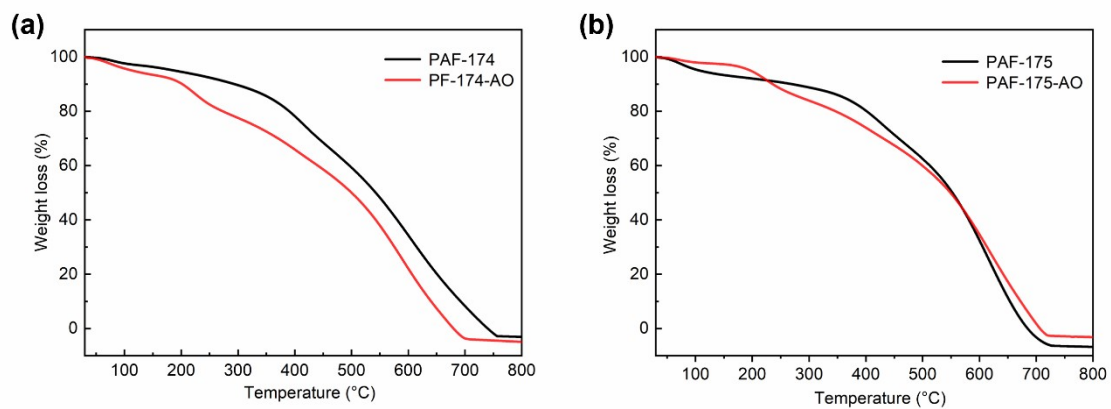


Figure S3. TGA curves of PAF-174, PAF-174-AO, PAF-175, and PAF-175-AO.

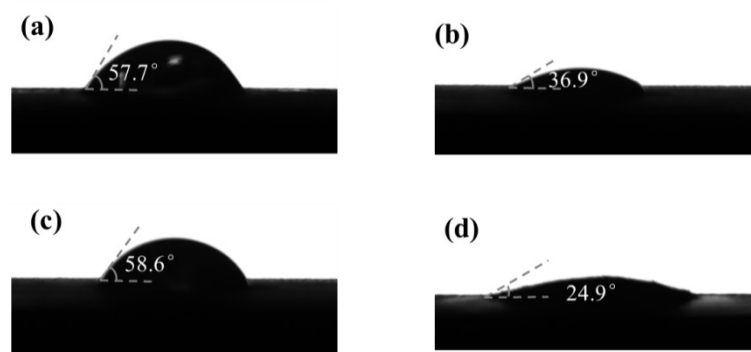


Figure S4. Water contact angles of PAF-174 (a), PAF-174 (b), PAF-175 (c), and PAF-175-AO (d).

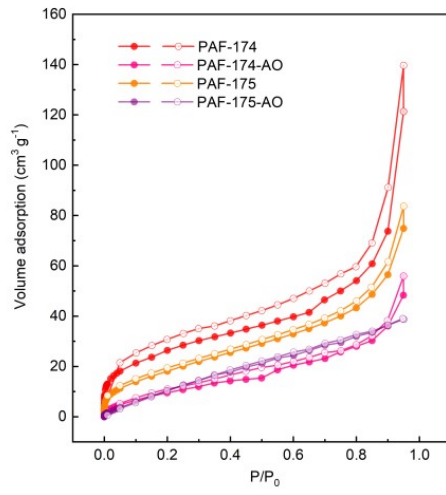


Figure S5. Nitrogen adsorption isotherms of PAF-174, PAF-174-AO, PAF-175, and PAF-175-AO.

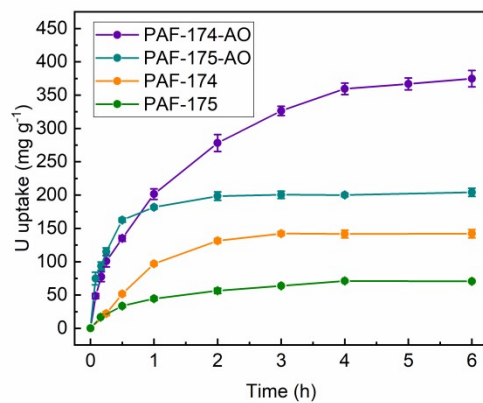


Figure S6. Adsorption capacity-time curves of PAF-174-AO, PAF-175-AO, PAF-174, and PAF-175 in aqueous solutions containing 10 ppm uranium.

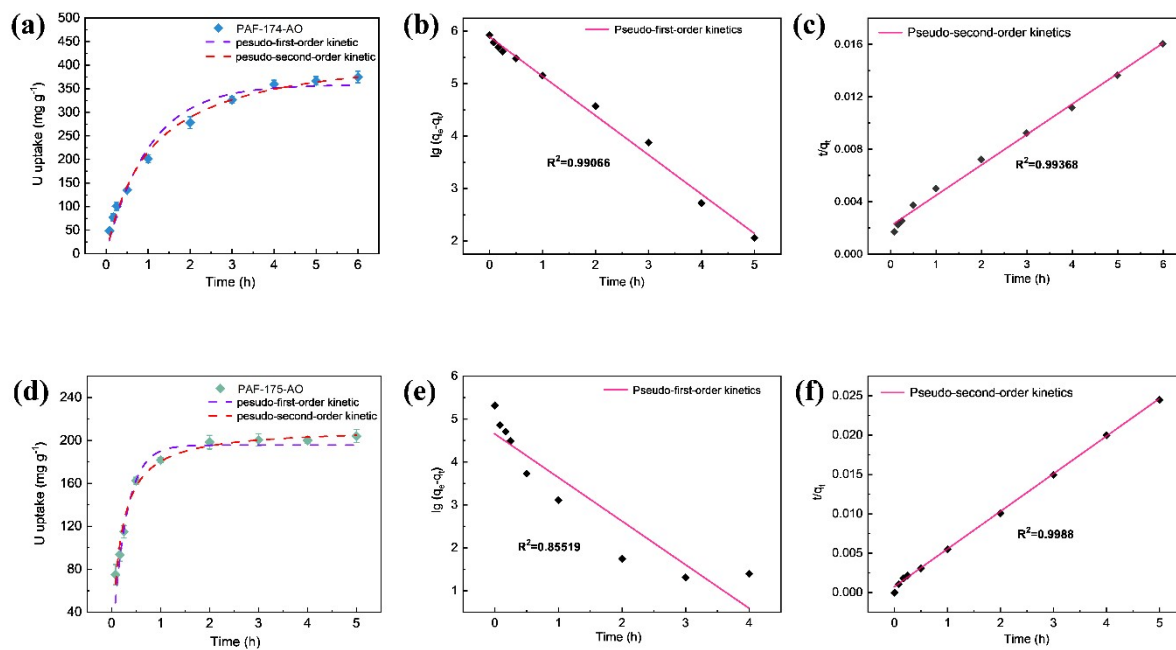


Figure S7. Kinetics for uranyl adsorption and the nonlinear fitting to the *pseudo-second-order* and *pseudo-first-order* kinetic models by PAF-174-AO and PAF-175-AO.

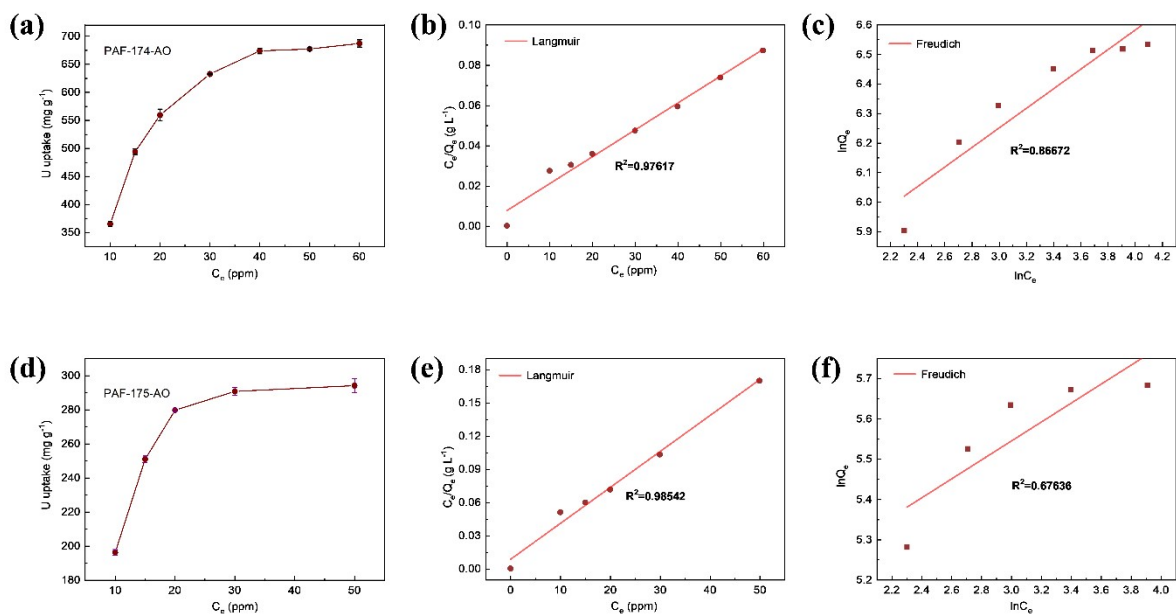


Figure S8. Langmuir and Freundlich models were used to fit the adsorption mechanism of PAF-174-AO and PAF-175-AO for uranyl at different concentrations.

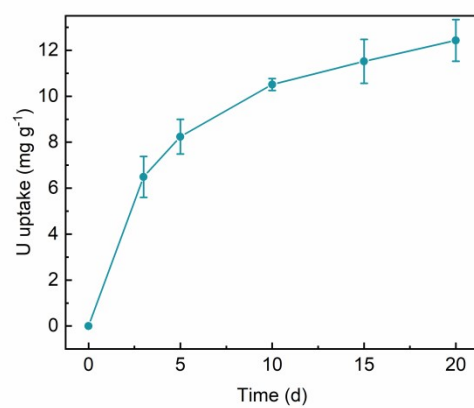


Figure S9. Adsorption properties of PAF-174-AO for uranyl ions after 20 days in natural seawater (initial uranium concentration ~3.4 ppb).

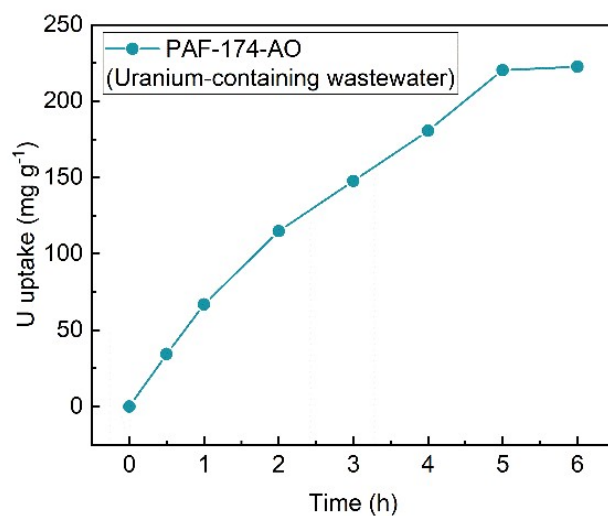


Figure S10. Adsorption characteristics of PAF-174-AO for uranyl ions in uranium-containing wastewater (initial uranium concentration ~10 ppm).

The coexisting ions (e.g., anions CO_3^{2-} , PO_4^{3-} , SO_4^{2-} , NO_3^- , Cl^- and cations Ca^{2+} , Al^{3+} , Fe^{3+} , Mg^{2+} , Na^+ , etc.) affect the adsorption performance of the materials for U(VI). The addition of 0.1 M, CO_3^{2-} , PO_4^{3-} , SO_4^{2-} , Cl^- , Ca^{2+} , Na^+ and Mg^{2+} , Fe^{3+} and Al^{3+} to a 10 ppm uranyl solution showed that the PAFs were highly stable and could still be applied in uranium-containing wastewater. The adsorption amount reached 222.5 mg g^{-1} .

Table S1. Time-dependent uranyl ion uptake of PAF-174-AO.

Time (min)	Uptake (mg g⁻¹)
0	0
5	48.5
10	77.4
15	100.7
30	135.1
60	201.5
120	278.2
180	326.4
240	359.5
300	366.9
360	374.7

Table S2. Comparison of ion selectivity of PAF-174-AO.

Ions	Capacity (mg g⁻¹)
UO ₂ ²⁺	297.5
Na ⁺	14.0
Fe ³⁺	37.9
VO ₃ ⁻	22.4
Zn ²⁺	30.6
Ni ²⁺	14.1
K ⁺	13.0
Ca ²⁺	23.4
Mg ²⁺	15.3
Cu ²⁺	25.6

Table S3. Kinetic parameters of PAF-174-AO and PAF-175-AO in the 10 ppm deionized water.

Materials	<i>Pseudo-first-order model</i>			<i>Pseudo-second-order model</i>		
	Q _e (mg g ⁻¹)	K ₁ (g mg ⁻¹ h ⁻¹)	R ²	Q _e (mg g ⁻¹)	K ₂ (g mg ⁻¹ h ⁻¹)	R ²
PAF-174-AO	361.1	0.75	0.9907	429.2	2.58×10 ⁻³	0.9937
PAF-175-AO	104.8	1.00	0.8552	208.8	3.48×10 ⁻²	0.9988

Table S4. U L3-edge EXAFS curve fitting parameters for PAF-174-AO-U.

U L3 edge	R- factor (%)	CN ₁ (U-O path)	R _{1(U-O path)} (Å)	$\sigma^2_{(U-O path)}$ (Å ²)
			1.80	1.76
		CN ₂ (U-O path)	R _{2(U-O/N path)} (Å)	$\sigma^2_{(U-O/N path)}$ (Å ²)
	0.028	1.43	2.27	0.001
		CN ₃ (U-O path)	R _{2(U-O/N path)} (Å)	$\sigma^2_{(U-O/N path)}$ (Å ²)
		3.33	2.45	0.001

Fits of the EXAFS spectrum were achieved by calculation of theoretical scattering paths with FEFF 6 using structure models obtained from the small molecules displayed in (Figure 5). Direct scattering paths were considered for all atoms in the uranyl first and second coordination sphere, while multiple scattering paths from the axial U=O were also included. A bottom-up approach was utilized to fit the data, where the coordination number (N), change in scattering half-path length (Δr), and mean squared relative displacement (σ^2) were local parameters, while amplitude reduction factor (S_0^2) was a global parameter to all scattering paths. Detailed parameters of scattering paths and fits were provided in Table S4.¹

Table S5. Comparison of adsorption affinity (K_d) of different adsorbents for uranyl ion by PAF-174-AO.

Material	K_d	Ref.
PAF-174-AO	1.08×10^6	This work
II-HPC	1.02×10^4	[2]
PAF-1-CH ₂ AO	1.05×10^6	[3]
MS@PIDO/Alg	1.98×10^4	[4]
MIPAF-11c	6.98×10^5	[5]
POP-oNH ₂ -AO	8.36×10^6	[6]
SMON-PAO	3.76×10^5	[7]
MISS-PAF-1	2.14×10^5	[8]

Table S6. Comparison of the uranium extraction performance from natural seawater.

Material	Capacity	Time	Ref.
PAF-174-AO	12.4	20	This
SSUP	12.33	3.5	[9]
BP-PAOfiber	11.76	30	[10]
SMON-PAO	9.59	56	[6]
PAO-PNMs	9.35	35	[11]
Zn ²⁺ -PAO	9.23	35	[12]
PAF-CS	8.92	56	[13]
PIDO NF	8.7	30	[14]
PPH-OP	7.12	56	[15]
POP-oNH ₂ -AO	4.36	56	[5]

Table S7. Cyanogenic functional group density of PAF-174 and PAF-175

Sample	Cyanide functional group content	Specific surface area	Cyanogenic functional group density
PAF-174	0.78 mmol g ⁻¹	96.5 m ² g ⁻¹	0.0081 mmol m ⁻²
PAF-175	0.66 mmol g ⁻¹	101.1 m ² g ⁻¹	0.0065 mmol m ⁻²

By calculating the number of grafted functional groups from the feeding ratio, it can be deduced that PAF-174-AO can obtain up to 0.78 mmol g⁻¹ of aminoxime group and PAF-175-AO can obtain up to 0.66 mmol g⁻¹ of aminoxime group, and according to this data, the saturated adsorption amount of PAF-174-AO is calculated to be 210.6 mg g⁻¹ and the saturated adsorption amount of PAF-175-AO is calculated to be 178.2 mg g⁻¹.

Table S8. Comparison of the uranium extraction performance from natural seawater.

Material	Specific surface area (m ² g ⁻¹)	Pore diameter (nm)	Seawater/Water Capacity (mg g ⁻¹)	Uranium concentration (ppm)	Natural seawater Capacity (mg g ⁻¹)	Time (days)	Ref.
PAF-174-AO	96.5	20	374.7	10	12.4	20	This
MIL-101-OA	2916	3.12	321	300	4.6	5	16
UiO-66-AO	711	NA	NA	NA	2.68	3d	17
COF-HHTF-AO	275	0.2	550	100	5.12	25	18
POP-oNH ₂ -AO	415	NA	290	10.3	4.36	56	5

References

1. B. Ravel and M. Newville, *J. Synchrotron. Rad.*, 2005, **12**, 537–541.
2. J. Zhu, Q. Liu, J. Liu, R. Chen, H. Zhang, J. Yu, M. Zhang, R. Li and J. Wang, *ACS Appl. Mater. Interfaces*, 2018, **10**, **34**, 28877–28886
3. B. Li, Q. Sun, Y. Zhang, C. Abney, B. Aguila, W. Lin and S. Ma, *ACS Appl. Mater. Interfaces*, 2017, **9**, **14**, 12511–12517.
4. D. Wang, J. Song, S. Lin, J. Wen, C. Ma, Y. Yuan, M. Lei, X. Wang, N. Wang and H. Wu, *Adv. Funct. Mater.*, 2019, **29**, 1901009.
5. Y. Yuan, Y. Yang, X. Ma, Q. Meng, L. Wang, S. Zhao and G. Zhu, *Adv. Mater.*, 2018, **30**, 1706507.
6. Q. Sun, B. Aguila, J. Perman, A. Ivanov, V. Bryantsev, L. Earl, C. Abney, L. Wojtas and S. Ma, *Nat. Commun.*, 2018, **9**, 1644.
7. Y. Yuan, S. Zhao, J. Wen, D. Wang, X. Guo, L. Xu, X. Wang and N. Wang, *Adv. Funct. Mater.*, 2018, **29**, 1805380.
8. Y. Yuan, Q. Meng, M. Faheem, Y. Yang, Z. Li, Z. Wang, D. Deng, F. Sun, H. He, Y. Huang, H. Sha and G. Zhu, *ACS Cent. Sci.*, 2019, **5**, 1432–1439.
9. Y. Yuan, Q. Yu, J. Wen, C. Li, Z. Guo, X. Wang and N. Wang, *Angew. Chem. Int. Ed.*, 2019, **58**, 11785.
10. Y. Yuan, B. Niu, Q. Yu, X. Guo, Z. Guo, J. Wen, T. Liu, H. Zhang and N. Wang, *Angew. Chem. Int. Ed.*, 2020, **59**, 1220.
11. S. Shi, Y. Qian, P. Mei, Y. Yuan, N. Jia, M. Dong, J. Fan, Z. Guo and N. Wang, *Nano Energy*, 2020, **71**, 104629.
12. B. Yan, C. Ma, J. Gao, Y. Yuan and N. Wang, *Adv. Mater.*, 2020, **32**, 1906615.
13. Z. Li, Q. Meng, Y. Yang, X. Zou, Y. Yuan and G. Zhu, *Chem. Sci.*, 2020, **11**, 4747–4752.
14. D. Wang, J. Song, J. Wen, Y. Yuan, Z. Liu, S. Lin, H. Wang, H. Wang, S. Zhao, X. Zhao, M. Fang, M. Lei, B. Li, N. Wang, X. Wang and H. Wu, *Adv. Energy Mater.*, 2018, **8**, 1802607.
15. Y. Yuan, Q. Yu, M. Cao, L. Feng, S. Feng, T. Liu, T. Feng, B. Yan, Z. Guo and N. Wang, *Nat. Sustain.*, 2021, **4**, 708–714.
16. H. Wu, F. Chi, S. Zhang, J. Wen, J. Xiong, S. Hu, *Micropor. Mesopor. Mat.*, 2019, **288**, 109567.
17. L. Chen, Z. Bai, L. Zhu, Lin. Zhang, Y. Cai, Y. Li, Wei. Liu, Y. Wang, L. Chen, J. Diwu, J. Wang, Z. Chai, S. Wang, *ACS Appl. Mater. Interfaces*. 2017, **9**, 32446–51.
18. G. Cheng, A. Zhang, Z. Zhao, Z. Chai, B. Hu, B. Han, Y. Ai, X. Wang, *Sci. Bull.*, 2021, **66**, 1944–2001.

